



## Neuroscience Research

journal homepage: [www.elsevier.com/locate/neures](http://www.elsevier.com/locate/neures)



### Research paper

# Immediate changes in transcription factors and synaptic transmission in the cochlea following acoustic trauma: A gene transcriptome study

Yukihide Maeda\*, Shin Kariya, Kensuke Uraguchi, Junko Takahara, Shohei Fujimoto, Akiko Sugaya, Kazunori Nishizaki

Department of Otolaryngology- Head and Neck Surgery, Okayama University Graduate School of Medicine, Dentistry and Pharmaceutical Sciences, 2-5-1 Shikata, Kita-Ku, Okayama, 700-8558, Japan

#### ARTICLE INFO

##### Article history:

Received 17 February 2020  
Received in revised form 18 April 2020  
Accepted 8 May 2020  
Available online xxx

##### Keywords:

Noise-induced hearing loss  
Mouse cochlea  
Transcription factor  
Neurotransmission  
RNA-seq  
DNA microarray  
Real-time RT-PCR  
Immunohistochemistry

#### ABSTRACT

Pathologic mechanisms in cochleae immediately following the onset of noise-induced hearing loss (NIHL) remain unclear. In this study, mice were exposed to 120 dB of octave band noise for 2 h to induce NIHL. Three hours after noise exposure, expression levels of the whole mouse genome in cochleae were analyzed by RNA-seq and DNA microarray. Differentially expressed genes (DEGs) exhibiting >2-fold upregulation or downregulation in noise-exposed cochleae compared to controls without noise exposure were identified. RNA-seq and microarray analyses identified 273 DEGs regulated at 3 h post-noise (51 upregulated and 222 downregulated). Bioinformatic analysis revealed that these DEGs were associated with the functional gene pathway "neuroactive ligand-receptor interaction" and included 28 genes encoding receptors for neurotransmitters such as gamma-aminobutyric acid and glutamate. Other DEGs included 25 genes encoding transcription factors. Downregulation of 4 neurotransmitter receptors (*Gabra3*, *Gabra5*, *Gabbr1*, *Gm1*) and upregulations of 5 transcription factors (*Atf3*, *Dbp*, *Helt*, *Maff*, *Nr1d1*) were validated by RT-PCR. The differentially regulated transcription factor *Atf3* immunolocalized to supporting cells and hair cells in the organ of Corti at 12-h post-noise. The present data serve as a basis for further studies aimed at developing medical treatments for acute sensorineural hearing loss.

© 2020 The Authors. Published by Elsevier B.V. This is an open access article under the CC BY-NC-ND license (<http://creativecommons.org/licenses/by-nc-nd/4.0/>).

## 1. Introduction

Exposure to intense noise can induce acute sensorineural hearing loss (SNHL) and a subsequent permanent threshold shift (PTS) in hearing levels. Noise-induced hearing loss (NIHL) is a major form of acute SNHL observed both in animal experiments and clinically. Animal models of NIHL are frequently used to experimentally explore therapeutic interventions to treat acute SNHL, such as treatment with glucocorticoids (Han et al., 2015), c-Jun N-terminal kinase inhibitor (Wang et al., 2007), and insulin-like growth factor-1 (Lee et al., 2007), which have already entered clinical trials (Han et al., 2017; Staecker et al., 2019; Yamahara et al., 2015).

During the acute phase of NIHL leading to PTS in cochleae, molecular pathologies such as inflammation, innate immune reactions, heat shock responses, intracellular stress pathway activation, and programmed and/or necrotic cell death are triggered, resulting in permanent damage to cochlear hair cells and spiral neurons

(Clifford et al., 2016; Kurabi et al., 2017). In order to develop effective therapeutic models for acute SNHL, it is important to understand how pathologic processes associated with NIHL are initially triggered in the cochlea immediately after noise trauma.

Gene transcriptome studies using next-generation sequencing (RNA-seq), DNA microarrays, and real-time RT-PCR analysis have been used to comprehensively investigate how the expression of over 20,000 mRNAs is regulated in the cochlear tissue of mice. The molecular pathologies of NIHL have been analyzed at the transcriptome level by examining mRNAs that encode proteins with known functions. In the 12- to 24 -h period following an intense noise exposure, inflammation and innate immune reactions are the primary functions associated with actively regulated mRNA pathways in murine cochleae (Yang et al., 2016; Maeda et al., 2017). However, few studies have analyzed the cochlear transcriptome immediately following acoustic trauma in mice (Alagramam et al., 2014). In this study, the cochlear gene transcriptome was analyzed as early as 3 h following noise-induced trauma in order to determine how the pathologic processes associated with NIHL are activated.

\* Corresponding author.

E-mail address: [yamayuki@cc.okayama-u.ac.jp](mailto:yamayuki@cc.okayama-u.ac.jp) (Y. Maeda).

<https://doi.org/10.1016/j.neures.2020.05.001>

0168-0102/© 2020 The Authors. Published by Elsevier B.V. This is an open access article under the CC BY-NC-ND license (<http://creativecommons.org/licenses/by-nc-nd/4.0/>).

## 2. Materials and methods

### 2.1. Induction of acute SNHL in mice following noise exposure

All animal experiments were performed in compliance with the ethical standards approved by the Okayama University Committee on the Use and Care of Animals (protocol numbers: OKU-2017012, OKU-2019324, principal investigator: Yukihide Maeda). Six to 7-week-old female C57BL/6 mice (postnatal day 44–52, Charles River, Yokohama, Japan) were used for the experiments.

Mice were exposed to 120 dB SPL of octave band noise (8.0–16.0 kHz) for 2 h, as described previously, with minor modifications (Maeda et al., 2013). It was previously confirmed that this intense noise exposure causes acute SNHL after 12 h ( $71.1 \pm 17.6$  dB SPL by click-ABR threshold, mean  $\pm$  S.D.) and 24 h ( $62.8 \pm 12.8$  dB), as well as a mild permanent threshold shift by 14 days ( $53.1 \pm 9.6$  dB) post-noise exposure, as compared to baseline levels before noise exposure ( $36.6 \pm 6.1$  dB) in 6-week-old female C57BL/6 mice (Maeda et al., 2018).

### 2.2. Dissection of cochlear tissue and RNA extraction

Three hours post-noise exposure, the mice were anesthetized with intraperitoneal ketamine (80 mg/kg) and xylazine (8 mg/kg), euthanized by cervical dislocation, and the cochlear tissues were promptly dissected. Cochlear tissues ( $n = 6$ , one cochlea per mouse) were collected and incubated in RNA later solution (Qiagen, Hilden, Germany) at 4 °C for 24 h and then stored frozen until RNA extraction. These tissues were designated the “Noise3 h” group in this study. Cochleae from mice not subjected to noise exposure were dissected and stored as baseline control sample ( $n = 6$ , one cochlea per mouse), and these tissues were designated the “Baseline” group in this study. The tissues were then homogenized, and total RNA was purified using an miRNeasy mini column (Qiagen). The quantity and quality of RNA extracted from the samples were assessed using NanoDrop One (Thermo Fisher Scientific, Waltham, MA) and an Agilent 2100 Bioanalyzer (Agilent Technologies, Santa Clara, CA). Per each cochlear tissue sample, 1.5–2.5 micrograms of total RNA with an RIN (RNA integrity number)  $>8.0$  was purified. The RNA samples were further processed for duplicate gene expression analyses by RNA-seq and DNA microarray.

### 2.3. Next-generation sequencing (RNA-seq)

Poly(A)-tailed mRNA samples were purified from total RNA samples using oligo dT magnetic beads with a NEBNext Poly(A) mRNA Magnetic Isolation Module (New England Biolabs, Ipswich, MA). A sequencing DNA library was synthesized using a NEBNext Ultra II Directional RNA Library Prep kit for Illumina (New England Biolabs). Sequencing was performed with 75-bp single-end reads using a NextSeq 500 platform (Illumina, San Diego, CA). RNA sequences were aligned to the mouse mm10 reference genome sequence, downloaded from the Illumina iGenomes ([http://jp.support.illumina.com/sequencing/sequencing\\_software/igenome.html](http://jp.support.illumina.com/sequencing/sequencing_software/igenome.html)), using Star 2.7.1 software (GitHub, Inc. <https://github.com/alexdobin/STAR>). Transcript sequences were annotated according to the RefSeq Gene database (<https://www.ncbi.nlm.nih.gov/refseq/>, April 1, 2013) using StrandNGS 3.2 software (Strand Life Sciences, Bangalore, Karnataka, India). Read counts were in the range 36,000,000 to 44,000,000 in the Noise3 h and Baseline samples. Read counts of the transcripts were normalized using the Trimmed Mean of M Values method, which represents the estimated expression level of each transcript. Gene transcripts were considered differentially expressed in the Noise3 h group as compared to the Baseline group

if the expression level was upregulated or downregulated with a  $>2$ -fold change.

### 2.4. DNA microarray

Total RNA (100 ng) was reverse-transcribed using oligo dT primers to synthesize cDNA. Cy3-labeled antisense cRNA was then synthesized with T7 RNA polymerase using a Low Input Quick Amp Labeling kit (Agilent). The Cy3-cRNA was hybridized to a SurePrint G3 Mouse GE microarray  $8 \times 60k$  ver. 2 (Agilent), which is an oligonucleotide array spotted with probes for over 27,000 mouse mRNAs. Fluorescence on the hybridized microarray was scanned using a DNA microarray scanner (Agilent) and quantified using Feature Extraction software (Agilent). Using GeneSpring ver. 14.9.1 software (Agilent), the signal intensity of each probe was normalized by 75th percentile shift normalization, and this value represented the expression level of each gene. Genes were considered differentially expressed in the Noise3 h group as compared to the Baseline group if the expression level was upregulated or downregulated with a  $>2$ -fold change.

### 2.5. Real-time RT-PCR

To validate the gene expression data obtained by the RNA-seq and DNA microarray analyses, real-time RT-PCR analysis was performed for 9 genes, encoding 4 neurotransmitter receptors and 5 transcription factors. RNA samples (500 ng) of the Noise3 h and Baseline groups were reverse-transcribed to synthesize a cDNA library using an RT<sup>2</sup> First Strand kit (Qiagen). Real-time PCR was performed using RT<sup>2</sup> SYBR Green qPCR Master mix (Qiagen) and primers specific for neurotransmitter receptor genes: *Gabra3* (gamma-aminobutyric acid [GABA] A receptor, subunit alpha 3; PPM04240A, RT<sup>2</sup> qPCR Primer Assay, Qiagen), *Gabra5* (GABAA receptor, subunit alpha 5; PPM36620A), *Gabbr1* (GABAA receptor, subunit beta 1; PPM04299A), and *Grm1* (glutamate receptor, metabotropic 1; PPM04275A), and the following transcription factor genes: *Atf3* (activating transcription factor 3; PPM04669C), *Dbp* (D site albumin promoter binding protein; PPM24977A), *Helt* (helt bHLH transcription factor; PPM31593A), *Maff* (v-maf musculoaponeurotic fibrosarcoma oncogene family, protein F; PPM30183B), and *Nr1d1* (nuclear receptor subfamily 1, group D, member 1; PPM05213E). The primers were specifically designed for the each gene and experimentally verified for real-time PCR analysis by Qiagen, Inc. The information of the gene-specific primers is provided at the Qiagen homepage (<https://geneglobe.qiagen.com/product-groups/rt2-qpcr-primer-assays>). A LightCycler480 system (Roche Molecular Diagnostics, Pleasanton, CA) was used for real-time RT-PCR analyses. Gene expression levels in each sample were calculated from  $\Delta$ Ct values normalized to the level of beta-2 microglobulin (PPM03562A) expression and presented as means  $\pm$  S.D. Differences in expression levels between the Noise3 h and Baseline groups were compared using the Student's *t*-test ( $n = 6$ ,  $p < 0.01$ ).

The expression level of *Atf3*, a transcription factor that controls the expression of genes involved in inflammation and innate immunity, was also analyzed in cochleae at 12 h post-noise trauma. A time-point of 12 h was selected because genes involved in inflammation and innate immunity are reportedly actively regulated in mice cochleae at 12 h post-noise trauma (Maeda et al., 2018, 2017).

### 2.6. Immunohistochemistry

Using samples obtained at 3 and 12 h after noise exposure, immunohistochemical analysis of paraffin-embedded sections of cochlear tissues was performed as previously described (Maeda et al., 2013). Samples from mice not subjected to noise exposure

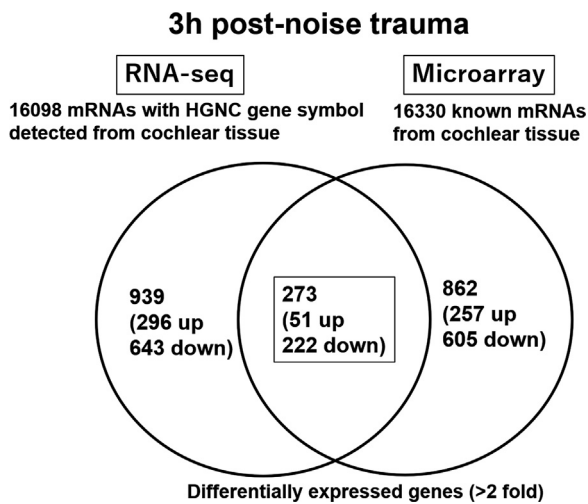


**Fig. 1.** Venn diagram showing differentially expressed genes (DEGs) detected by RNA-seq and microarray analyses.

Circles indicate DEGs exhibiting more than 2-fold upregulation or downregulation in the Noise3 h group compared to the Baseline group. A total of 273 genes were finally identified as DEGs based on matching results of the RNA-seq and DNA microarray analyses.

served as baseline controls. Cochlear immunolocalization of a transcription factor differentially regulated by noise trauma, *Atf3*, was visualized using rabbit polyclonal anti-*Atf3* antibody (HPA001562, SIGMA, St. Louis, MO, USA) according to the ABC method (Vectastain Elite ABC kit, Vector Laboratories, Burlingame, CA, USA). Paraffin-embedded sections were incubated with the primary antibody (diluted 1/100) at 4 °C overnight. Sections incubated without primary antibody served as negative controls. Immunofluorescent visualization of specific *Atf3* signal was also performed using Alexa Fluor 568 donkey anti-rabbit IgG (A10042, Thermo Fisher Scientific, diluted 1/200) at 4 °C for 30 m. Light and fluorescent microscopic images in this paper were obtained using a fluorescent microscope (BX-51-54, Olympus, Tokyo).

### 2.7. Data analysis

In each RNA-seq and DNA microarray experiment, lists of genes exhibiting a more than 2-fold change in expression level between the Noise3 h and Baseline groups were generated. The identified genes are represented by the official gene symbols designated by the HUGO Gene Nomenclature Committee (HGNC, <http://www.genenames.org/>). Differentially expressed genes (DEGs) exhibiting either upregulation or downregulation (>2-fold change in expression) in the Noise3 h group, as compared to the Baseline group, were identified by comparing the results of the RNA-seq and DNA microarray analyses. DEGs exhibited a >2-fold change in expression in both the RNA-seq and microarray analyses. The biological pathways and molecular functions associated with the identified DEGs were investigated using KEGG (Kyoto Encyclopedia of Genes and Genomics) pathway analysis and Gene Ontology (GO) term analysis with David Bioinformatics Resources 6.8 (<https://david.ncifcrf.gov/>) (Huang et al., 2009a, b).

### 2.8. Data availability

The raw RNA-seq data described in this report were deposited in the NCBI Sequence Read Archive (<http://www.ncbi.nlm.nih.gov/sra>) and are available through the accession number (SRA: PRJNA573404). Raw DNA microarray data were deposited in the NCBI Gene Expression Omnibus (<http://www.ncbi.nlm.nih.gov/geo>) under the accession number (GEO: GSE137817).

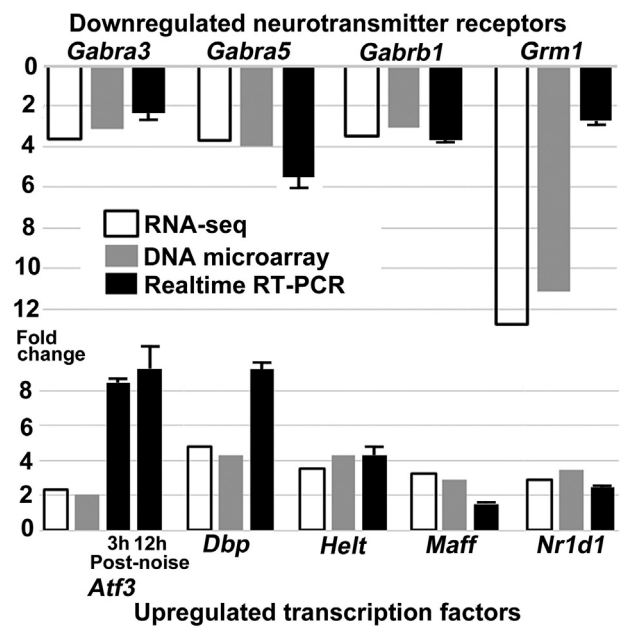


**Fig. 2.** Real-time RT-PCR validation of the expression of gamma-aminobutyric acid (GABA) A receptor, a glutamate receptor and transcription factors.

Real-time RT-PCR confirmed that *Gabra3* (GABAA receptor, subunit alpha 3;  $2.33 \pm 0.40$ -fold change, mean  $\pm$  S.D.), *Gabra5* (GABAA receptor, subunit alpha 5;  $5.52 \pm 0.60$ -fold change), *Gabrb1* (GABAA receptor, subunit beta 1;  $3.71 \pm 0.16$ -fold change), and *Grm1* (glutamate receptor, metabotropic 1;  $2.71 \pm 0.26$ -fold change) were significantly downregulated in the Noise3 h group compared to the Baseline group ( $n = 6$ ,  $p < 0.01$ ). *Atf3* (activating transcription factor 31;  $8.44 \pm 0.31$ -fold change), *Dbp* (D site albumin promoter binding protein1;  $11.23 \pm 0.46$ -fold change), *Helt* (helt bHLH transcription factor1;  $4.34 \pm 0.56$ -fold change), *Maff* (v-maf musculoaponeurotic fibrosarcoma oncogene family, protein F1;  $1.49 \pm 0.03$ -fold change), and *Nr1d1* (nuclear receptor subfamily 1, group D, member 11;  $2.48 \pm 0.10$ -fold change) were significantly upregulated in the Noise3 h group compared to the Baseline group ( $n = 6$ ,  $p < 0.01$ ). Based on matching results of RNA-seq, DNA microarray, and real-time RT-PCR analyses, these neurotransmitter receptor and transcription factor genes were identified as differentially regulated in the Noise3h group compared to the Baseline group. *Atf3* was also upregulated in cochleae at 12 h post-noise trauma compared to the Baseline group ( $13.3 \pm 1.35$ -fold change,  $n = 6$ ,  $p < 0.01$ ). Therefore, *Atf3* was upregulated in cochleae at both 3 and 12 h post-noise trauma.

## 3. Results

### 3.1. Identification of DEGs by RNA-seq and microarray

As illustrated in Fig. 1, in vivo RNA-seq detected the expression of a total of 16,098 genes in cochlear tissues of the Noise3 h and Baseline groups. These genes were expressed in the tissues as known mRNAs identified by official HGNC gene symbols. A total of 939 genes were differentially expressed, either upregulated (296 genes) or downregulated (643 genes), exhibiting a more than 2-fold change by comparison of the Noise3 h and Baseline groups. By comparison, the in vivo DNA microarray analysis detected the expression of a total of 16,330 known mRNAs in cochlear tissue. A total of 862 genes were differentially expressed, either upregulated (257 genes) or downregulated (605 genes), exhibiting a more than 2-fold change by comparison of the Noise and Baseline groups. Among the 939 genes exhibiting a more than 2-fold change in expression by RNA-seq, 273 genes were verified as upregulated (51 genes) or downregulated (222 genes) in comparing the Noise3 h and Baseline groups by DNA microarray. These 273 genes were therefore designated DEGs.

The symbols and names of the DEGs identified in this study are tabulated in the Supplementary Material of this paper. The biological pathways and molecular functions associated with these DEGs were further investigated using a web-based genome database: David Bioinformatics Resources.

### 3.2. Genome bioinformatics analysis of DEGs

KEGG pathways denote biological processes that involve large sets of genes. A cut-off value of 0.05 was used for the *p*-value and false discovery rate (FDR). If a subset of genes of interest is identified in abundance in a KEGG pathway with a *p*-value < 0.05 and FDR < 0.05, these genes are considered as significantly enriching this pathway with a specific biological function.

Table 1 (upper rows) shows KEGG pathways significantly enriched in genes differentially expressed between the Noise 3 h and Baseline groups. DEGs identified in cochleae at 3 h after noise trauma most significantly enriched the KEGG pathway “Neuroactive ligand-receptor interaction”. Thirty-two DEGs were actively regulated in this KEGG pathway, and these genes are listed in Table 2. Twenty-eight of these genes encode receptors for synaptic transmission by neurotransmitters: GABA, glutamate, glycine, epinephrine, norepinephrine, acetylcholine, dopamine, serotonin, and neurotensin; as well as receptors for various hormones: calcitonin, prolactin, and somatostatin. All of the DEGs identified in the neuroactive ligand-receptor interaction pathway, with the exception of the calcitonin receptor, were downregulated at 3 h post-noise trauma.

The second most abundantly enriched KEGG pathway was “Nicotine addiction”, but all of the DEGs regulated in the “Nicotine addiction” pathway were also identified in the “Neuroactive ligand-receptor interaction” pathway (data not shown). Other highly enriched KEGG pathway in DEGs between the Noise3 h and Baseline groups included “GABAergic synapse”, “Glutamatergic synapse”, “Dopaminergic synapse”, and “Retrograde endocannabinoid signaling”, which are closely associated with synaptic neurotransmission. The “PPAR signaling pathway” was also significantly enriched; this pathway mediates intranuclear signaling via peroxisome proliferator-activated receptors (i.e., PPARs).

Gene Ontology (GO) terms denote the classification of a large set of multiple genes based on function. A cut-off value of 0.05 was used for both the *p*-value and FDR in GO analyses. If a specific GO term is frequently associated in the database with the functions of genes of interest at a *p*-value < 0.05 and FDR < 0.05, this subset of genes is considered to be involved in molecular functions represented by that GO term. The exact definitions of GO terms are available from the European Bioinformatics Institute (<https://www.ebi.ac.uk/QuickGO/>).

Table 1 (lower rows) tabulates GO terms significantly associated with molecular functions of the DEGs identified in this study. The top 5 significant GO terms of the cochlear DEGs at 3 h post-noise trauma are “Extracellular ligand-gated ion channel activity”, “GABAA receptor activity”, “Chloride channel activity”, “Ion channel activity”, and “Hormone activity”. These molecular functions are associated with neural signal processing and humoral communication in the nervous system and closely related to the “Neuroactive ligand-receptor interaction” KEGG pathway associated with these DEGs. It is notable that a large number of the DEGs were identified as transcriptional regulators with the GO terms “Sequence-specific DNA binding” (23 genes), “RNA polymerase II regulatory region sequence-specific DNA binding” (11 genes), and “Transcription factor activity” (25 genes). Table 3 shows the 25 DEGs encoding transcription factors that were either upregulated (9 genes) or downregulated (16 genes) in the cochlea at 3 h post-noise trauma.

It was previously shown that inflammation and innate immune reactions are the primary functions of genes actively regulated in cochleae at 12–24 h post-noise trauma (Yang et al., 2016; Maeda et al., 2017). However in the present study, no KEGG pathways or GO terms related to inflammation or innate immunity were identified with a *p*-value < 0.05 and FDR < 0.05 as major functions of cochlear DEGs as early as 3 h after noise exposure. Among genes

encoding inflammatory cytokines and other immune signaling molecules, *Ccl2* (chemokine [C-C motif] ligand 2), *Ccl7* (chemokine [C-C motif] ligand 7), *Cxcl10* (chemokine [C-X-C motif] ligand 10), *Il6* (interleukin 6), and *Fkbp5* (FK506 binding protein 5) were upregulated with a >2-fold change in the cochlea at 3 h post-noise trauma (tabulated in Supplementary Material).

### 3.3. Real-time RT-PCR

As shown in Fig. 2, real-time RT-PCR analyses confirmed that 4 neurotransmitter genes, *Gabra3* (2.33 ± 0.40-fold change, mean ± S.D.), *Gabra5* (5.52 ± 0.60-fold change), *Gabrb1* (3.71 ± 0.16-fold change), and *Grm1* (2.71 ± 0.26-fold change), were significantly downregulated in the Noise3 h group as compared to the Baseline group (*p* < 0.01). Five transcription factor genes, *Atf3* (8.44 ± 0.31-fold change, mean ± S.D.), *Dbp* (11.23 ± 0.46-fold change), *Helt* (4.34 ± 0.56-fold change), *Maff* (1.49 ± 0.03-fold change), and *Nr1d1* (2.48 ± 0.10-fold change), were significantly upregulated in the Noise3 h group as compared to the Baseline group (*p* < 0.01). As the results of RNA-seq, microarray, and real-time RT-PCR analyses matched, these neurotransmitter receptor and transcription factor genes were determined to be differentially regulated in the cochlea at 3 h after noise-induced trauma.

*Atf3* expression was significantly upregulated in cochleae at 12 h post-noise trauma compared to the Baseline group (13.3 ± 1.35-fold change, *p* < 0.01). The *Atf3* gene was upregulated in cochleae at both 3 and 12 h post-noise trauma.

### 3.4. Immunohistochemistry

As shown in Fig. 3, *Atf3* expression was detected in the sensory epithelium at 3 and 12 h post-noise exposure. *Atf3* expression was distinctly observed in the supporting cells and hair cells in the organ of Corti at 12 h post-noise. *Atf3* expression was undetectable in sections of cochlear tissue taken from Baseline-group mice not subjected to noise exposure, however.

## 4. Discussion

The present RNA-seq and DNA microarray analyses identified 273 DEGs either upregulated or downregulated among the whole genome of cochlear tissue at 3 h after acoustic trauma. A strong concordance has been reported between data obtained from RNA-seq analyses and a specific type of DNA microarray, the Agilent oligonucleotide microarray (Nault et al., 2015). Combining RNA-seq and DNA microarray analyses allows for high-throughput validation of gene transcriptome data, as these data are verified using two different technologies.

Previously, Alagramam et al. analyzed the gene expression change associated with the early onset of NIHL using DNA microarray and showed that mitogen-activated protein kinase signaling was modulated in cochleae at 1 h post-noise exposure. Although they used a different protocol for the data analysis from ours, they demonstrated that *Atf3* was an upregulated transcription factor in cochleae with NIHL, which is consistent with the data in this paper (Alagramam et al., 2014).

In our data, as many as 32 genes encoding neurotransmitter receptors for synaptic transmission as well as receptors for hormones in the “Neuroactive ligand-receptor interaction” pathway were downregulated at 3 h post-noise trauma. Genes encoding neurotransmitter receptors in both excitatory synapses (e.g., glutamate receptor) and inhibitory synapses (e.g., GABAA receptor) were downregulated in the cochlea. As a validation of the RNA-seq and DNA microarray data, downregulation of 3 GABAA receptor genes (*Gabra3*, *Gabra5*, and *Gabrb1*) and 1 metabotropic glutamate receptor gene (*Grm1*) was verified by real-time RT-PCR analysis. These

**Table 1**

Kyoto Encyclopedia of Genes and Genomes (KEGG) pathways and Gene Ontology (GO) terms significantly associated with the differentially expressed genes (DEGs).

|   | Gene count | p-value(<0.05) | FDR(<0.05) |
|---|------------|----------------|------------|
| Neuroactive ligand-receptor interaction   | 32         | 4.0E-19        | 6.7E-17    |
| Nicotine addiction  | 12         | 7.5E-12        | 6.3E-10    |
| Retrograde endocannabinoid signaling  | 16         | 2.0E-11        | 1.1E-09    |
| GABAergic synapse   | 15         | 2.4E-11        | 1.0E-09    |
| Morphine addiction  | 14         | 8.0E-10        | 2.7E-08    |
| Circadian entrainment   | 10         | 1.3E-05        | 3.7E-04    |
| Glutamatergic synapse   | 10         | 4.8E-05        | 1.1E-03    |
| PPAR signaling pathway  | 8          | 1.7E-04        | 3.6E-03    |
| Dopaminergic synapse  | 9          | 8.1E-04        | 1.5E-02    |
| Circadian rhythm  | 5          | 1.1E-03        | 1.8E-02    |
| Regulation of lipolysis in adipocytes   | 6          | 1.5E-03        | 2.2E-02    |
| Amphetamine addiction   | 6          | 3.0E-03        | 4.2E-02    |
| Functions of DEGs: Gene Ontology terms  |            |                |            |
| Extracellular ligand-gated ion channel activity   | 13         | 1.7E-13        | 7.6E-11    |
| GABA-A receptor activity  | 9          | 6.8E-11        | 1.6E-08    |
| Chloride channel activity   | 12         | 7.6E-10        | 1.2E-07    |
| Ion channel activity  | 14         | 5.8E-07        | 6.6E-05    |
| Hormone activity  | 11         | 3.0E-06        | 2.7E-04    |
| Symporter activity  | 10         | 2.2E-05        | 1.7E-07    |
| Sequence-specific DNA binding   | 23         | 5.5E-05        | 3.6E-03    |
| Protein dimerization activity   | 11         | 2.8E-04        | 1.6E-02    |
| Glutamate binding   | 4          | 6.4E-04        | 3.2E-02    |
| RNA polymerase II regulatory region sequence-specific DNA binding   | 11         | 9.1E-04        | 4.0E-02    |
| Transcription factor activity, sequence-specific DNA binding  | 25         | 9.8E-04        | 4.0E-02    |
| Glycine binding   | 4          | 1.0E-03        | 3.7E-02    |
| Transmitter-gated ion channel activity  | 3          | 1.1E-03        | 3.7E-02    |
| Transcriptional activator activity, RNA polymerase II core promotor proximal region sequence-specific binding | 12         | 1.2E-03        | 3.8E-02    |
| Receptor binding  | 15         | 1.6E-03        | 4.6E-02    |

The upper table shows KEGG gene pathways significantly enriched with DEGs between the Noise3 h group and the Baseline group. The KEGG pathways indicate the functions of the identified DEGs. The cut-off values for significantly enriched KEGG pathways were set at  $p$ -value <0.05 and false discovery rate (FDR) <0.05. The lower table shows GO terms significantly associated with the functions of the DEGs. GO terms indicate the molecular functions of the DEGs. The exact definitions of these GO terms are available from the European Bioinformatics Institute (<http://www.ebi.ac.uk/QuickGO/>). The cut-off values for significantly associated GO terms with DEGs were set at  $p$ -value <0.05 and FDR < 0.05.

results suggest that dysregulation of synaptic transmission is a major pathologic characteristic of the cochlear transcriptome in the immediate early period 3 h post–noise trauma. These observations also have significant implications with respect to the development of therapeutic models of acute SNHL. For example, systemic injections of Piribedil, a dopamine agonist, and/or Memantine, a glutamate open channel blocker, were shown to decrease ABR threshold shifts and loss of inner hair cell (IHC)-auditory nerve synapses following noise trauma in rodents (Altschuler et al., 2016). Systemic injection of Muscimol, a GABAA agonist, attenuated ABR threshold shifts and swelling of the afferent dendrites in contact with IHCs following acoustic overexposure in mice (Murashita et al., 2007). Dysregulation of synaptic transmission may be a relatively common pathological process in cochleae with acute SNHL, including not only NIHL but also drug-induced SNHL. It was reported that gentamicin administration to mice caused reduction in the ribbon synapse number of the inner hair cell (Liu et al., 2013).

It was previously demonstrated that genes associated with inflammation and innate immunity are the most actively regulated genes in cochleae at 12–24 h post-noise trauma (Maeda et al., 2017; Yang et al., 2016). However, in the present data, collected as early as 3 h after noise exposure, no major pathways associated with inflammation or innate immunity were identified as significantly enriched in DEGs in the cochlea during this early post-trauma time point. Among inflammation- and immunity-related genes, *Ccl2*, *Ccl7*, *Cxcl10*, *Il6*, and *Fkbp5* were upregulated in the cochlea at 3 h post-noise trauma. *Ccl2*, *Ccl7*, and *Cxcl10* encode chemokines found to be upregulated in the cochlea at both 3 and 12 h post-noise trauma, as shown in both the present study and our previous experiments (Maeda et al., 2018). IL-6 is a proinflammatory cytokine that mediates the acute phase response during inflammation. It was previously reported that IL-6 expression was upregulated in the spiral

ligament of the cochlea at 3 h post-noise trauma (Fujioka et al., 2006). *Fkbp5* mediates intracellular signaling of the glucocorticoid receptor. Dexamethasone administered to mice intratympanically was shown to upregulate *Fkbp5* expression in the cochlea at 12 h post-administration (Maeda et al., 2012). These genes thus encode key molecules involved in the early processes of cochlear inflammation following noise-induced trauma.

In the early period 3 h after noise-induced trauma, 25 transcription factors were found to be actively regulated in the cochlea. These transcription factors may control a variety of cellular processes, including inflammation, innate immunity, neural plasticity, apoptosis, autophagy, induction of nitric oxide synthase, cell cycle regulation, and cell proliferation, and migration, according to information from the NCBI Online Mendelian Inheritance in Man database (<https://www.ncbi.nlm.nih.gov/omim>). Real-time RT-PCR results further indicated that the expression of 5 transcription factor genes (*Atf3*, *Dbp*, *Helt*, *Maff*, and *Nr1d1*) was significantly upregulated in the cochlea at 3 h after noise-induced trauma. *Atf3* controls transcriptional responses of inflammation and innate immunity to cellular stresses triggered by toll-like receptor signaling (De Nardo, 2015). MAFF transcription factor positively regulates the expression of inflammatory cytokine genes, including *CCL2* and *IL6*, in cultured human cell lines (Saliba et al., 2019). *Nr1d1* inactivates transcription of *Nlrp3* in the inflamed mice with inflammatory colitis (Wang et al., 2018). These immediate transcription factors may control inflammation and innate immune reactions in the cochlea during the acute period of NIHL. In our study, *Atf3* expression was localized in the supporting cells and hair cells in the organ of Corti at 12 h post-noise exposure. Thus, the transcriptional modulation of inflammation- and immunity-related genes involves, at least in part, the sensory epithelium of the cochlea. The present cochlear gene transcriptome

**Table 2**  
List of differentially expressed genes (DEGs) in the “Neuroactive ligand-receptor interaction” pathway.

| Gene symbol (HGNC) | Gene name  | Fold change by RNA-seq | Fold change by microarray | Regulation 3 h post noise trauma |
|--------------------|--|------------------------|---------------------------|----------------------------------|
| <i>Calcr</i>       | Calcitonin receptor  | 2.067                  | 2.219                     | Up                               |
| <i>Adcyap1r1</i>   | Adenylate cyclase activating polypeptide 1 receptor 1      | 2.414                  | 2.399                     | Down                             |
| <i>Adrb3</i>       | Adrenergic receptor, beta 3                                | 4.697                  | 3.965                     | Down                             |
| <i>Cga</i>         | Glycoprotein hormones, alpha subunit                       | 9.223                  | 8.015                     | Down                             |
| <i>Chrm4</i>       | Cholinergic receptor, nicotinic, delta polypeptide         | 3.306                  | 3.213                     | Down                             |
| <i>Drd5</i>        | Dopamine receptor D5                                       | 8.799                  | 13.620                    | Down                             |
| <i>Fshb</i>        | Follicle stimulating hormone beta                          | 6.613                  | 5.235                     | Down                             |
| <i>Gabra2</i>      | Gamma-aminobutyric acid (GABA) A receptor, subunit alpha 2 | 2.274                  | 2.044                     | Down                             |
| <i>Gabra3</i>      | Gamma-aminobutyric acid (GABA) A receptor, subunit alpha 3 | 3.608                  | 3.118                     | Down                             |
| <i>Gabra4</i>      | Gamma-aminobutyric acid (GABA) A receptor, subunit alpha 4 | 3.275                  | 2.899                     | Down                             |
| <i>Gabra5</i>      | Gamma-aminobutyric acid (GABA) A receptor, subunit alpha 5 | 3.720                  | 3.999                     | Down                             |
| <i>Gabra6</i>      | Gamma-aminobutyric acid (GABA) A receptor, subunit alpha 6 | 2.698                  | 2.800                     | Down                             |
| <i>Gabbr1</i>      | Gamma-aminobutyric acid (GABA) A receptor, subunit beta 1  | 3.500                  | 3.043                     | Down                             |
| <i>Gabbrd</i>      | Gamma-aminobutyric acid (GABA) A receptor, subunit delta   | 2.956                  | 2.341                     | Down                             |
| <i>Gabrg1</i>      | Gamma-aminobutyric acid (GABA) A receptor, subunit gamma 1 | 3.527                  | 2.670                     | Down                             |
| <i>Gabrg3</i>      | Gamma-aminobutyric acid (GABA) A receptor, subunit gamma 3 | 4.409                  | 2.308                     | Down                             |
| <i>Glr1a1</i>      | Glycine receptor, alpha 1 subunit                          | 115.615                | 24.457                    | Down                             |
| <i>Glr1a2</i>      | Glycine receptor, alpha 2 subunit                          | 5.463                  | 7.115                     | Down                             |
| <i>Grid2</i>       | Glutamate receptor, ionotropic, delta 2                    | 2.718                  | 3.141                     | Down                             |
| <i>Grin2a</i>      | Glutamate receptor, ionotropic, NMDA2A (epsilon 1)         | 10.057                 | 4.207                     | Down                             |
| <i>Grin2b</i>      | Glutamate receptor, ionotropic, NMDA2B (epsilon 2)         | 3.942                  | 2.097                     | Down                             |
| <i>Grm1</i>        | Glutamate receptor, metabotropic 1                         | 12.760                 | 11.157                    | Down                             |
| <i>Grm3</i>        | Glutamate receptor, metabotropic 3                         | 5.370                  | 4.282                     | Down                             |
| <i>Grm5</i>        | Glutamate receptor, metabotropic 5                         | 7.410                  | 4.874                     | Down                             |
| <i>Htr2b</i>       | 5-hydroxytryptamine (serotonin) receptor 2B                | 5.403                  | 2.009                     | Down                             |
| <i>Htr2c</i>       | 5-hydroxytryptamine (serotonin) receptor 2C                | 2.253                  | 2.720                     | Down                             |
| <i>Ntsr2</i>       | Neurotensin receptor 2                                     | 2.933                  | 3.182                     | Down                             |
| <i>Plg</i>         | Plasminogen  | 3.254                  | 2.042                     | Down                             |
| <i>Prl</i>         | Prolactin  | 11.799                 | 11.364                    | Down                             |
| <i>Prlr</i>        | Prolactin receptor   | 3.568                  | 4.482                     | Down                             |
| <i>Sstr1</i>       | Somatostatin receptor 1                                    | 2.194                  | 2.663                     | Down                             |
| <i>Sstr3</i>       | Somatostatin receptor 3                                    | 5.138                  | 2.375                     | Down                             |

Bioinformatics analyses indicated that genes differentially expressed between the Noise3 h group and Baseline group were functionally associated with the KEGG “Neuroactive ligand-receptor interaction” pathway. For example, 9 GABAA receptor genes and 6 glutamate receptor genes were downregulated in the Noise3 h group compared to the Baseline group.

**Table 3**  
List of differentially expressed genes (DEGs) encoding transcription factors.

| Gene symbol (HGNC) | Gene name  | Fold change by RNA-seq | Fold change by microarray | Regulation 3 h post noise trauma |
|--------------------|--|------------------------|---------------------------|----------------------------------|
| <i>Atf3</i>        | Activating transcription factor 3                                | 2.351                  | 2.082                     | Up                               |
| <i>Dbp</i>         | D site albumin promoter binding protein                          | 4.810                  | 4.299                     | Up                               |
| <i>Fos</i>         | FBJ osteosarcoma oncogene  | 2.502                  | 2.093                     | Up                               |
| <i>Fosb</i>        | FBJ osteosarcoma oncogene B                                      | 4.861                  | 2.296                     | Up                               |
| <i>Fos11</i>       | fos-like antigen 1   | 11.430                 | 6.819                     | Up                               |
| <i>Helt</i>        | helt bHLH transcription factor                                   | 3.501                  | 4.293                     | Up                               |
| <i>Maff</i>        | v-maf musculoaponeurotic fibrosarcoma oncogene family, protein F | 3.245                  | 2.927                     | Up                               |
| <i>Nr1d1</i>       | Nuclear receptor subfamily 1, group D, member 1                  | 2.871                  | 3.443                     | Up                               |
| <i>Nr1d2</i>       | Nuclear receptor subfamily 1, group D, member 2                  | 2.005                  | 2.485                     | Up                               |
| <i>Arntl</i>       | Aryl hydrocarbon receptor nuclear translocator-like              | 2.237                  | 3.798                     | Down                             |
| <i>Cdkn2a</i>      | Cyclin-dependent kinase inhibitor 2A                             | 3.306                  | 2.604                     | Down                             |
| <i>Elf5</i>        | E74-like factor 5  | 2.256                  | 2.007                     | Down                             |
| <i>Eomes</i>       | Eomesodermin homolog   | 2.961                  | 2.429                     | Down                             |
| <i>Lbx1</i>        | Ladybird homeobox homolog 1                                      | 8.962                  | 2.334                     | Down                             |
| <i>Nkx2-2</i>      | NK2 transcription factor related, locus 2                        | 2.105                  | 2.086                     | Down                             |
| <i>Nkx6-2</i>      | NK6 homeobox 2   | 2.698                  | 2.610                     | Down                             |
| <i>Npas2</i>       | Neuronal PAS domain protein 2                                    | 4.037                  | 3.502                     | Down                             |
| <i>Olig1</i>       | Oligodendrocyte transcription factor 1                           | 2.818                  | 2.697                     | Down                             |
| <i>Olig2</i>       | Oligodendrocyte transcription factor 2                           | 3.869                  | 2.499                     | Down                             |
| <i>Pax6</i>        | Paired box gene 6  | 3.446                  | 6.546                     | Down                             |
| <i>Ppara</i>       | Peroxisome proliferator activated receptor alpha                 | 2.308                  | 2.301                     | Down                             |
| <i>Rfx4</i>        | Regulatory factor X, 4 (influences HLA class II expression)      | 2.357                  | 2.169                     | Down                             |
| <i>Sox3</i>        | SRY-box containing gene 3  | 6.616                  | 5.803                     | Down                             |
| <i>St18</i>        | Suppression of tumorigenicity 18                                 | 2.260                  | 2.285                     | Down                             |
| <i>Tbx5</i>        | T-box 5  | 2.204                  | 5.256                     | Down                             |

Bioinformatics analyses indicated that genes differentially expressed between the Noise3 h group and Baseline group encoded transcription factors. The functions of these DEGs were associated with GO terms related to transcription factor activity.

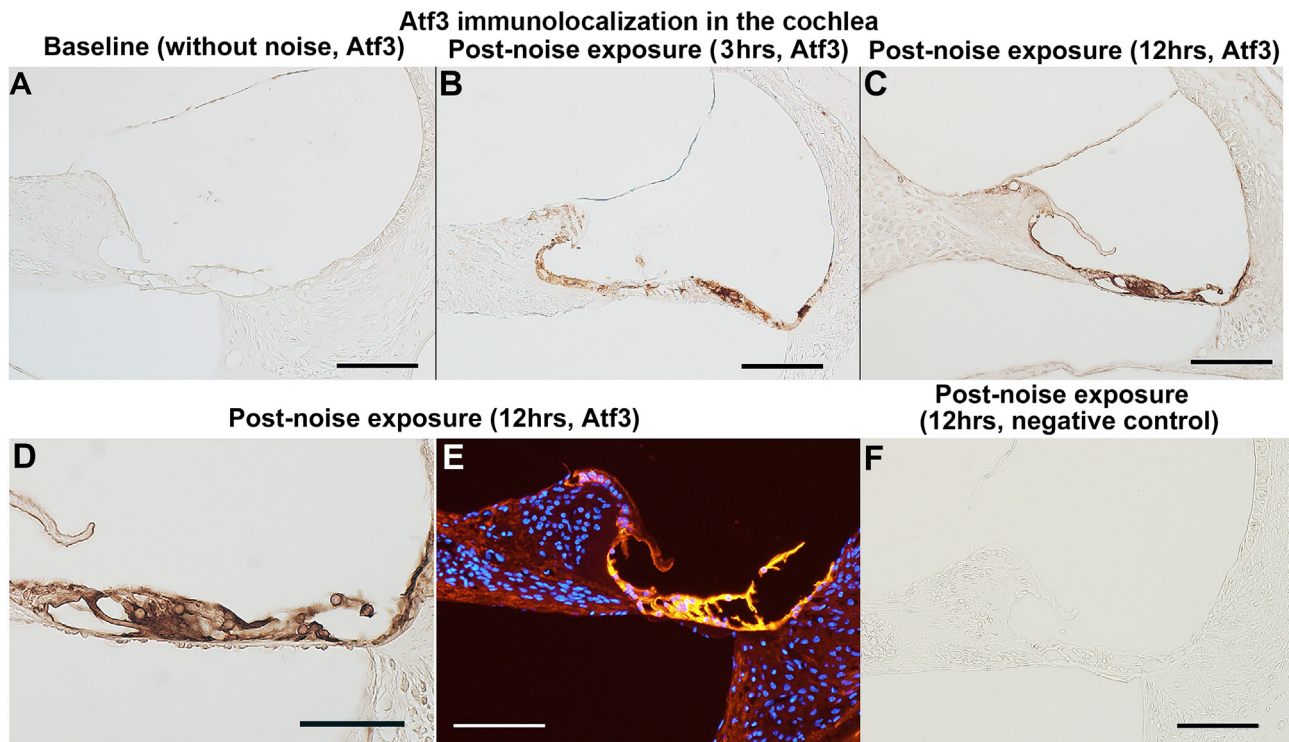


**Fig. 3.** Cochlear immunolocalization of activating transcription factor 3 (Atf3) protein.

Atf3 expression was detected in the sensory epithelium at 3 and 12 h post-noise exposure (B and C). Atf3 expression was distinctly observed in the supporting cells and hair cells in the organ of Corti at 12 h post-noise (C–E).

Atf3 expression was undetectable in the Baseline cochlear sections from mice not subjected to noise exposure (A), and the negative control section from the noise-exposed mouse (F). Figure (D) is the magnified image of (C). In Figure (E), blue indicates the nuclear staining by DAPI. Atf3 immunoreactivity is detected as the red and yellow signals. The intense Atf3 signal appears as the yellow signal. Scale bars indicate 100  $\mu\text{m}$  (A, B, C, E, F) and 50  $\mu\text{m}$  (D). (For interpretation of the references to colour in this figure legend, the reader is referred to the web version of this article.)

data clarify the early pathologic processes of NIHL and serve as a foundation for further basic and clinical studies aimed at developing medical treatments for acute SNHL.

### Funding and disclosure

The authors declare no competing financial interests. This work was supported by JSPS KAKENHI Grant Numbers JP16K11181 and JP19K09845. JSPS (Japan Society for the Promotion of Science) has no roles in study design; in the collection, analysis and interpretation of data; in the writing of the report; and in the decision to submit the article for publication.

### Declaration of Competing Interest

None.

### Acknowledgment

None.

### Appendix A. Supplementary data

Supplementary material related to this article can be found, in the online version, at doi:<https://doi.org/10.1016/j.neures.2020.05.001>.

### References

Alagramam, K.N., Stepanyan, R., Jamesdaniel, S., Chen, D.H., Davis, R.R., 2014. Noise exposure immediately activates cochlear mitogen-activated protein kinase signaling. *Noise Health* 16, 400–409.

Altschuler, R.A., Wys, N., Prieskorn, D., Martin, C., DeRemer, S., Bledsoe, S., Miller, J.M., 2016. Treatment with Piribedil and memantine reduces noise-induced loss of inner hair cell synaptic ribbons. *Sci. Rep.* 6, 30821.

Clifford, R.E., Hoffer, M., Rogers, R., 2016. The genomic basis of noise-induced hearing loss: a literature review organized by cellular pathways. *Otol. Neurotol.* 37, e309–316.

De Nardo, D., 2015. Toll-like receptors: activation, signaling and transcriptional modulation. *Cytokine* 74, 181–189.

Fujioka, M., Kanzaki, S., Okano, H.J., Masuda, M., Ogawa, K., Okano, H., 2006. Proinflammatory cytokines expression in noise-induced damaged cochlea. *J. Neurosci. Res.* 83, 575–583.

Han, M.A., Back, S.A., Kim, H.L., Park, S.Y., Yeo, S.W., Park, S.N., 2015. Therapeutic effect of dexamethasone for noise-induced hearing loss: systemic versus intratympanic injection in mice. *Otol. Neurotol.* 36, 755–762.

Han, X., Yin, X., Du, X., Sun, C., 2017. Combined intratympanic and systemic use of steroids as a first-line treatment for sudden sensorineural hearing loss: a meta-analysis of randomized, controlled trials. *Otol. Neurotol.* 38, 487–495.

Huang, D.W., Sherman, B.T., Lempicki, R.A., 2009a. Bioinformatics enrichment tools: paths toward the comprehensive functional analysis of large gene lists. *Nucleic Acids Res.* 37, 1–13.

Huang, D.W., Sherman, B.T., Lempicki, R.A., 2009b. Systematic and integrative analysis of large gene lists using DAVID bioinformatics resources. *Nature Protoc* 4, 44–57.

Kurabi, A., Keithley, E.M., Housley, G.D., Ryan, A.F., Wong, A.C., 2017. Cellular mechanisms of noise-induced hearing loss. *Hear. Res.* 349, 129–137.

Lee, K.Y., Nakagawa, T., Okano, T., Hori, R., Ono, K., Tabata, Y., Lee, S.H., Ito, J., 2007. Novel therapy for hearing loss: delivery of insulin-like growth factor 1 to the cochlea using gelatin hydrogel. *Otol. Neurotol.* 28, 976–981.

Liu, K., Jiang, X., Shi, C., Shi, L., Yang, B., Shi, L., Xu, Y., Yang, W., Yang, S., 2013. Cochlear inner hair cell ribbon synapse is the primary target of ototoxic aminoglycoside stimuli. *Mol. Neurobiol.* 48, 647–654.

Maeda, Y., Fukushima, K., Kariya, S., Orita, Y., Nishizaki, K., 2012. Intratympanic dexamethasone up-regulates Fkbp5 in the cochlea of mice in vivo. *Acta Otolaryngol.* 132, 4–9.

Maeda, Y., Fukushima, K., Omichi, R., Kariya, S., Nishizaki, K., 2013. Time courses of changes in phospho- and total- MAP kinases in the cochlea after intense noise exposure. *PLoS One* 8, e58775.

Maeda, Y., Omichi, R., Sugaya, A., Kariya, S., Nishizaki, K., 2017. Cochlear transcriptome following acoustic trauma and dexamethasone administration identified by a combination of RNA-seq and DNA microarray. *Otol. Neurotol.* 38, 1032–1042.

- Maeda, Y., Kariya, S., Omichi, R., Noda, Y., Sugaya, A., Fujimoto, S., Nishizaki, K., 2018. Targeted PCR array analysis of genes in innate immunity and glucocorticoid signaling pathways in mice cochleae following acoustic trauma. *Otol. Neurotol.* 39, e593–e600.
- Murashita, H., Tabuchi, K., Sakai, S., Uemaetomari, I., Tsuji, S., Hara, A., 2007. The effect of a GABAA agonist muscimol on acoustic injury of the mouse cochlea. *Neurosci. Lett.* 418, 18–21.
- Nault, R., Fader, K.A., Zacharewski, T., 2015. RNA-Seq versus oligonucleotide array assessment of dose-dependent TCDD-elicited hepatic gene expression in mice. *BMC Genomics* 16, 373.
- Saliba, J., Coutaud, B., Solovieva, V., Lu, F., Blank, V., 2019. Regulation of CXCL1 chemokine and CSF3 cytokine levels in myometrial cells by the MAFF transcription factor. *J. Cell. Mol. Med.* 23, 2517–2525.
- Staecker, H., Jokovic, G., Karpishchenko, S., Kienle-Gogolok, A., Krzyzaniak, A., Lin, C.D., Navratil, P., Tzvetkov, V., Wright, N., Meyer, T., 2019. Efficacy and safety of AM-111 in the treatment of acute unilateral sudden Deafness-A double-blind, randomized, placebo-controlled phase 3 study. *Otol. Neurotol.* 40, 584–594.
- Wang, J., Ruel, J., Ladrech, S., Bonny, C., van de Water, T.R., Puel, J.L., 2007. Inhibition of the c-Jun N-terminal kinase-mediated mitochondrial cell death pathway restores auditory function in sound-exposed animals. *Mol. Pharmacol.* 71, 654–666.
- Wang, S., Lin, Y., Yuan, X., Li, F., Guo, L., Wu, B., 2018. REV-ERBalpha integrates colon clock with experimental colitis through regulation of NF-kappaB/NLRP3 axis. *Nat. Commun.* 9, 4246.
- Yamahara, K., Yamamoto, N., Nakagawa, T., Ito, J., 2015. Insulin-like growth factor 1: a novel treatment for the protection or regeneration of cochlear hair cells. *Hear. Res.* 330, 2–9.
- Yang, S., Cai, Q., Vethanayagam, R.R., Wang, J., Yang, W., Hu, B.H., 2016. Immune defense is the primary function associated with the differentially expressed genes in the cochlea following acoustic trauma. *Hear. Res.* 333, 283–294.